NASA Technical Memorandum 102202

Numerical Simulation of Viscous Incompressible Flows

D. Kwak, S. Rogers, S. Yoon, and M. Rosenfeld, Ames Research Center, Moffett Field, California
J. L. C. Chang, Rockwell International, Canoga Park, California

September 1989

National Aeronautics and
Space Administration

Ames Research Center
Moffett Field, California 94035

NUMERICAL SIMULATION OF VISCOUS INCOMPRESSIBLE FLOWS

D. Kwak, S. Rogers, S. Yoon, M. Rosenfeld
NASA Ames Research Center, Moffett Field, CA
and
J.L.C. Chang
Rocketdyne, Rockwell International, Canoga Park, CA

SUMMARY

This paper discusses incompressible Navier-Stokes solution methods and their applications to three-dimensional flows. A brief review of existing methods is given followed by a description of recent progress on development of three-dimensional generalized flow solvers. Emphasis is placed on primitive variable formulations which are most promising and flexible for general three-dimensional computations of viscous incompressible flows. Both steady- and unsteady-solution algorithms are discussed. Finally, examples of real world applications of these flow solvers are given.

KEY WORDS Incompressible Flow, Navier Stokes Equations, Finite Differences

1. INTRODUCTION

Viscous incompressible flows have played an important role both in basic fluid dynamics research and in industrial applications. In two-dimensional studies, incompressible flows have been a convenient choice for laboratory experiments such as low speed wind tunnel or water tank experiments. Computational study of these flow problems have been performed for several decades and naturally various viscous incompressible flow solution methods have been developed. In many realistic engineering applications, incompressible flows are also encountered. Naming a few, there are problems related to low speed aerodynamics and hydrodynamics such as the flow around high lift devices, the flow around submerged vehicles, flow through impeller passages, mixing of the flow in chemical reactors, coolant flow in nuclear reactors, and certain biofluid problems. There are algorithmic simplifications as well as geometric modeling involved in computing these flows. Furthermore, significant

physical modeling is also required, such as turbulence modeling for high Reynolds number flows. Therefore, numerical computation of these flows, especially in three dimensions, becomes both an art and a science.

Until the recent past, computational flow simulation has not been a critical element in resolving many engineering problems. For instance, impellers, automobiles, submarines, and chemical reactors have been designed reasonably well by empirical means. As technologies advance, modern flow devices tend toward a more compact and highly efficient design. Therefore, the approach relying on empiricism and simplified analysis becomes inadequate for resolving problems associated with those devices requiring advanced analysis. For example, in analyzing and redesigning the current Space Shuttle main engine (SSME) power head, computational simulations became an economical and time-saving supplement to experimental data. There are vast numbers of other real-world problems which demand accurate viscous, incompressible flow solutions, such as rocket-engine fuel flow, flow through an impeller and blood flow through a ventricular assist device. Therefore, it is of considerable interest to have a computational fluid dynamics (CFD) capability for simulating these important applications as an alternative to analytical or empirical approaches.

The present report summarizes our recent progress in developing viscous incompressible flow solvers and their applications to real world problems. Among various approaches, the primitive variable formulation is considered to be the most promising for 3-D applications, and is therefore emphasized. In the present paper, brief descriptions of various methods are given followed by some computed results.

2. SOLUTION METHODS

2.1 Formulation

The incompressible Navier-Stokes equations for 3-D flows can be written in curvilinear coordinates, (ξ, η, ζ), as

$$\frac{\partial}{\partial t}\hat{u} = -\frac{\partial}{\partial \xi_i}(\hat{e}_i - \hat{e}_{vi}) = -\hat{r} \tag{2.1}$$

$$\frac{\partial}{\partial \xi_i}\left(\frac{U_i - (\xi_i)_t}{J}\right) = 0 \tag{2.2}$$

where

$$\hat{u} = \frac{1}{J}\begin{bmatrix} u \\ v \\ w \end{bmatrix}$$

$$\hat{e}_i = \frac{1}{J}\begin{bmatrix} (\xi_i)_x p + uU_i \\ (\xi_i)_y p + vU_i \\ (\xi_i)_z p + wU_i \end{bmatrix}, \quad \hat{e_{v_i}} = \frac{\nu}{J}\nabla\xi_i \cdot (\nabla\xi_l \frac{\partial}{\partial\xi_l})\begin{bmatrix} u \\ v \\ w \end{bmatrix} \tag{2.3}$$

$$U_i = (\xi_i)_t + (\xi_i)_x u + (\xi_i)_y v + (\xi_i)_z w$$

$$J = \text{Jacobian of the transformation}$$

Here, t is the time, x_i the Cartesian coordinates, u_i the corresponding velocity components, p the pressure, and ν the total kinematic viscosity. A constant viscosity is assumed for simplicity and all variables are nondimensionalized by a reference velocity and length scale.

The major difference between the incompressible and the compressible Navier-Stokes formulation is the lack of a time derivative term in the continuity equation. Therefore, satisfying the mass conservation equation is the primary issue in solving the above set of equations. Among various techniques, the primitive variable formulation, namely, using pressure and velocities as dependent variables, is chosen for convenience and flexibility in 3-D applications. A brief review is given next on methods using primitive variables.

2.2 Previous Work Using Primitive Variables

The solution method using primitive variables has been frequently chosen in 3-D problems. Among many variations of this approach, several commonly used methods are summarized here.

2.2.1 Methods Based on Pressure Iteration

MAC Method

Perhaps the first primitive variable method is the marker-and-cell (MAC) method developed by Harlow and Welch (1965). In this method, the pressure is used as a mapping parameter to satisfy the continuity equation. By taking the divergence of the momentum equation, the Poisson equation for pressure is obtained. The usual computational procedure involves choosing the pressure field at the current time step such that continuity is satisfied at the next time step. To satisfy the continuity equation in grid space, the divergence of the gradient form of the Laplacian operator has to be used. This is essential in satisfying the mass conservation in grid space (see Kwak, 1989). The original MAC method is based on a staggered arrangement on a 2-D Cartesian grid. The staggered grid avoids

odd-even point decoupling of the pressure encountered in a regular grid (Gresho and Sani, 1987). However, these properties become unclear in the case of generalized coordinates. Ever since its introduction, numerous variations of the MAC method have been devised and successful computations have been made. Many more examples can be found in the literature, for example, by Roach (1972), Ferziger (1987), Orszag and Israelli (1974).

The major drawback of this method is the large computing time required for solving the Poisson equation for pressure. When the physical problem requires a very small time step, the penalty paid for an iterative solution procedure for the pressure may be tolerable.

SIMPLE Method

In the MAC method, the strict requirement of obtaining the correct pressure for a divergence-free velocity field at each step slows down the overall computational efficiency significantly. However, for a steady-state solution, the pressure-iterations procedure can be simplified such that it requires only a few iterations at each time step. The best known example of this approach is the SIMPLE method (Semi-Implicit Method for Pressure-Linked Equations) developed by Caretto et al. (1972), see also Patankar and Spalding (1972) or Patankar (1980).

The method begins with a guessed pressure, which is usually assumed to be the pressure at the previous step. Then the momentum equation is solved to get an intermediate velocity. Then pressure and the velocity corrections are obtained from a simplified momentum equation. The procedure in essence results in a simplified Poisson equation for pressure, which can be solved iteratively line-by-line. The unique feature of this method comes from the simple way of estimating the velocity correction. Despite this simplification, many computations have been done successfully. Further details of SIMPLE and other variations can be found in the literature, for example, see Patankar (1980).

Fractional-Step Method

The fractional-step method can be used for time-dependent computations (see, Chorin, 1968; Yanenko, 1971; Marchuk, 1975). The common application of this method involves two steps. The first step is to solve for an auxilary velocity field using the momentum equation in which the pressure-gradient term can be estimated from the pressure in the previous time-step (see Dwyer, 1986) or can be excluded entirely (see Kim and Moin, 1985). In the second step, the pressure is computed in such a way as to map the auxiliary velocity onto a divergence-free velocity field.

One particular aspect of the fractional step method requiring special care is the inter-

mediate boundary conditions. Orszag et al. (1986) discussed this extensively. As with other pressure based methods, the efficiency of the fractional step method depends on the Poisson solver. A multigrid acceleration, which is physically consistent with the elliptic field, is one possiblility to enhance the computational efficiency.

2.2.2 Methods Based on Compressible Flow Algorithms

Recent advances in the state of the art in CFD have been made in conjunction with compressible flow computations. Therefore, the compressible flow algorithms are of significant interest. To apply these algorithms, the artificial compressibility method of Chorin (1967) can be used. In this formulation, the continuity equation is modified by adding a time-derivative of the pressure term. Together with the unsteady momentum equations, this forms a hyperbolic-parabolic type of time-dependent system of equations. Thus, fast implicit schemes developed for compressible flows, such as the approximate-factorization scheme by Beam and Warming (1978) and the implicit lower-upper symmetric-Gauss-Seidel (LU-SGS) scheme by Yoon and Jameson (1987), can be implemented. Various applications evolved from this concept have been reported for obtaining steady-state solutions (e.g., Steger and Kutler, 1977; Kwak et al. 1986, Chang et al., 1984,1988; Choi and Merkle, 1985). To obtain time-dependent solutions using this method, an iterative procedure can be applied in each physical time step such that the continuity equation is satisfied. Merkle and Athavale (1987) and Rogers and Kwak (1988, 1989) reported successful computations using this pseudotime iteration approach.

This method, known as the pseudocompressibility method, has been extensively utilized in developing several incompressible Navier-Stokes codes at NASA Ames Research Center. Further discussion of this method is given next.

2.3 Pseudocompressibility Method

As introduced in the previous section, the pseudocompressibility method can be used for both steady and time-dependent problems. In this section, several solution procedures using this method are outlined.

2.3.1 Steady-State Formulation

The pseudocompressibility relation is introduced by adding a time derivative of pressure to the continuity equation, which results in

$$\frac{\partial}{\partial \tau}\hat{D} = -\frac{\partial}{\partial \xi_i}(\hat{E}_i - \hat{E}_{v_i}) = -\hat{R} \tag{2.4}$$

where $\hat{R}$ is the right-hand-side of the momentum equation and can be defined as the residual for the steady state computations, and where

$$\hat{D} = \frac{D}{J} = \frac{1}{J}\begin{bmatrix} p \\ u \\ v \\ w \end{bmatrix}, \hat{E}_i = \begin{bmatrix} \beta(U_i - (\xi_i)_t)/J \\ \hat{e}_i \end{bmatrix}, \hat{E}_{vi} = \begin{bmatrix} 0 \\ \hat{e_{v_i}} \end{bmatrix} \tag{2.5}$$

In the steady-state formulation the equations are to be marched in a time-like fashion until the divergence of velocity converges to zero. The time variable for this process no longer represents physical time. Therefore in the momentum equations t is replaced with τ, which can be thought of as a pseudotime or iteration parameter.

2.3.2 Steady-State Algorithm Using Approximate Factorization

An unfactored implicit scheme can be written in delta form as follows:

$$\begin{aligned} &\left\{I + \frac{h}{2}J\left[\delta_\xi(\hat{A}^n - \Gamma_1) + \delta_\eta(\hat{B}^n - \Gamma_2) + \delta_\zeta(\hat{C}^n - \Gamma_3)\right]\right\}(D^{n+1} - D^n) \\ &= -\Delta\tau J\left[\delta_\xi(\hat{E} - \hat{E}_v)^n + \delta_\eta(\hat{F} - \hat{F}_v)^n + \delta_\zeta(\hat{G} - \hat{G}_v)^n\right] \end{aligned} \tag{2.6}$$

where

$$\Gamma_1 D^{n+1} = (\frac{\nu}{J})\nabla\xi \cdot (\nabla\xi\frac{\partial}{\partial\xi} + \nabla\eta\frac{\partial}{\partial\eta} + \nabla\zeta\frac{\partial}{\partial\zeta})I_m\frac{\partial D}{\partial\xi}..\text{etc.}$$

$$h = \Delta\tau \quad \text{for trapezoidal, or} \quad 2\Delta\tau \quad \text{for Euler}$$

$$I_m = diag[0,1,1,1]$$

At this point it should be noted that the notation of the form $[\delta_\xi(A - \Gamma)]D$ refers to $\frac{\partial}{\partial\xi}(AD) - \frac{\partial}{\partial\xi}(\Gamma D)$. The flux vector E_i and the Jacobian matrices are represented by $\hat{E}_i = \hat{E}, \hat{F}, \text{or } \hat{G}$ and $\hat{A}_i = \hat{A}, \hat{B}, \text{or } \hat{C}$ for $i = 1, 2, \text{or } 3$, respectively.

ADI scheme

The solution of equation (2.6) would involve a formidable matrix inversion problem. With the use of an ADI (alternating direction implicit) type scheme, the problem could be reduced to the inversion of three matrices of small bandwidth, for which there exist some efficient solution algorithms. One particular ADI form used here is known as approximate factorization (AF) (Beam and Warming, 1978). Using this form, the governing equation becomes

$$L_\xi L_\eta L_\zeta(D^{n+1} - D^n) = RHS \tag{2.7}$$

where

$$L_{\xi_i} = \left[I + \frac{\Delta\tau}{2} J^{n+1} \delta_{\xi_i} (\hat{A}_i{}^n - \gamma_i) \right]$$

γ_i represents the orthogonal part of the viscous term and RHS is the right-hand side of equation (2.6) where the entire viscous term is used to maintain the accuracy of the solution. When second-order central differencing is used, the solution to this problem becomes the inversion of three block tridiagonal matrices, which can be diagonalized (see Rogers et al., 1987).

LU-SGS scheme

Recently, Yoon and Jameson (1987) developed an implicit lower-upper symmetric-Gauss-Seidel (LU-SGS) scheme for the compressible Euler and Navier-Stokes equations. A similar scheme is devised for the pseudocompressible formulation (Yoon and Kwak, 1989). This LU-SGS scheme is not only unconditionally stable but completely vectorizable in three-dimensions. Spacial differencing can be either central or upwind depending on the numerical dissipation model which augments the finite volume method (Yoon and Kwak, 1988). This scheme is described below.

Starting from an unfactored implicit scheme similar to equation (2.6)

$$\begin{aligned} &\left\{ I + \frac{h}{2} \left[\delta_\xi \hat{A} + \delta_\eta \hat{B} + \delta_\zeta \hat{C} \right] \right\} (D^{n+1} - D^n) \\ &\quad = -\Delta t \left[\delta_\xi (\hat{E} - \hat{E}_v) + \delta_\eta (\hat{F} - \hat{F}_v) + \delta_\zeta (\hat{G} - \hat{G}_v) \right] \end{aligned} \tag{2.6'}$$

The LU-SGS implicit factorization scheme can be derived as

$$L_l L_d{}^{-1} L_u = RHS \tag{2.8}$$

where

$$\begin{aligned} L_l &= I + \frac{h}{2} (\delta^-{}_\xi \hat{A}^+ + \delta^-{}_\eta \hat{B}^+ + \delta^-{}_\zeta \hat{C}^+ - \hat{A}^- - \hat{B}^- - \hat{C}^-) \\ L_d &= I + \frac{h}{2} (\hat{A}^+ - \hat{A}^+ + \hat{B}^+ - \hat{B}^- + \hat{C}^+ - \hat{C}^-) \\ L_u &= I + \frac{h}{2} (\delta^+{}_\xi \hat{A}^- + \delta^+{}_\eta \hat{B}^- + \delta^+{}_\zeta \hat{C}^- + \hat{A}^+ + \hat{B}^+ + \hat{C}^+) \end{aligned}$$

where $\delta^-{}_\xi$ and $\delta^+{}_\xi$ are backward and forward difference operator respectively. In the framework of the LU-SGS algorithm, a variety of schemes can be developed by different choices of numerical dissipation models and Jacobian matrices of the flux vectors. Further details of this method will be given in a later report (Yoon and Kwak, 1989).

2.3.3 Time-Accurate Formulation

Time-dependent calculation of incompressible flows are especially time consuming due to the elliptic nature of the governing equations. Therefore, it is particularly desirable to develop computationally efficient methods by implementing a fast algorithm and by utilizing computer characteristics such as vectorization and parallel processing. In this section, a time-accurate method using pseudocompressibility developed by Rogers and Kwak (1988, 1989) is briefly introduced.

In this formulation the time derivatives in the momentum equations are differenced using a second-order, three-point, backward-difference formula

$$\frac{3\hat{u}^{n+1} - 4\hat{u}^{n} + \hat{u}^{n-1}}{2\Delta t} = -\hat{r}^{n+1} \tag{2.9}$$

where the superscript n denotes the quantities at time $t = n\Delta t$ and $\hat{r}$ is the right-hand side given in equation (2.1). To solve equation (2.9) for a divergence free velocity at the $n+1$ time level, a pseudo-time level is introduced and is denoted by a superscript m. The equations are iteratively solved such that $\hat{u}^{n+1,m+1}$ approaches the new velocity $\hat{u}^{n+1}$ as the divergence of $\hat{u}^{n+1,m+1}$ approaches zero. To drive the divergence of this velocity to zero, the following artificial compressibility relation is introduced:

$$\frac{p^{n+1,m+1} - p^{n+1,m}}{\Delta\tau} = -\beta\nabla \cdot \hat{u}^{n+1,m+1} \tag{2.10}$$

where τ denotes pseudo-time and β is an artificial compressibility parameter. Combining equation (2.10) with the momentum equations gives

$$\begin{aligned} &I_{t\tau}(\hat{D}^{n+1,m+1} - \hat{D}^{n+1,m}) \\ &= -\hat{R}^{n+1,m+1} - \frac{I_m}{\Delta t}(1.5\hat{D}^{n+1,m} - 2\hat{D}^{n} + 0.5\hat{D}^{n-1}) \end{aligned} \tag{2.11}$$

where $\hat{D}$ is the same vector defined in equation (2.5) and $\hat{R}$ is the same residual vector defined in equation (2.4). Also appearing in this equation is $I_{t\tau}$ which is a diagonal matrix and I_m which is a modified identity matrix given by

$$I_{t\tau} = \text{diag}\left[\frac{1}{\Delta\tau}, \frac{1.5}{\Delta t}, \frac{1.5}{\Delta t}, \frac{1.5}{\Delta t}\right], \quad I_m = diag[0,1,1,1]$$

Finally, the residual term at the $m+1$ pseudo-time level is linearized, giving the following equation in delta form

$$\begin{aligned} &\left[\frac{I_{t\tau}}{J} + \left(\frac{\partial\hat{R}}{\partial D}\right)^{n+1,m}\right](D^{n+1,m+1} - D^{n+1,m}) \\ &= -\hat{R}^{n+1,m} - \frac{I_m}{\Delta t}(1.5\hat{D}^{n+1,m} - 2\hat{D}^{n} + 0.5\hat{D}^{n-1}) \end{aligned} \tag{2.12}$$

The derivatives of the viscous fluxes in this vector are approximated using second-order central differences. The convective flux terms can be discretized using central differences. However, this will require numerical dissipation terms for stability. Since, in the pseudocompressible formulation, the governing equations are changed into the hyperbolic-parabolic type, some of the upwind differencing schemes which have recently been developed for the compressible Euler and Navier-Stokes equations by a number of authors (i.e. Roe, 1981; Chakravarthy and Osher, 1985; Steger and Warming, 1981; Harten et al, 1983) can be utilized. In the present work, Roe's method (1981) was used in differencing the convective terms by an upwind method. Then the set of numerical equations is solved using a nonfactored line relaxation scheme similar to that employed by MacCormack (1985).

Further information on the pseudocompressibility method can be found in the References.

2.4 Fractional Step Method

In the previous section, the pseudocompressibility approach was described for obtaining time-accurate solutions. An alternative approach is the pressure iteration method. Among several choices in this category, the fractional step method allows flexibility in combining various operator splitting techniques. Among its numerous variants, a general 3-D fractional step procedure developed by Rosenfeld et. al. (1988, 1989) is described in this section.

2.4.1 Formulation

The equations governing the flow of isothermal, constant density incompressible, viscous fluids in a time-dependent control volume with the face $\mathbf{S}(t)$ and volume $V(t)$ are written in integral form for the conservation of mass

$$\frac{\partial V}{\partial t} + \oint_S d\mathbf{S} \cdot (\mathbf{u} - \mathbf{v}) = 0 \tag{2.13}$$

and for the conservation of momentum

$$\frac{\partial}{\partial t} \int_V \mathbf{u}\, dV = \oint_S d\mathbf{S} \cdot \bar{T} \tag{2.14}$$

where t is the time, $\mathbf{u}$ is the velocity vector, $\mathbf{v}$ is the surface element velocity resulting from the motion of the grid, and $d\mathbf{S}$ is a surface area vector. The tensor $\bar{T}$ is given by

$$\bar{T} = -(\mathbf{u} - \mathbf{v})\mathbf{u} - pI + \nu \left(\nabla \mathbf{u} + (\nabla \mathbf{u})^T\right) \tag{2.15}$$

where $\nabla \mathbf{u}$ is the gradient of $\mathbf{u}$ and $(\,)^T$ is the transpose operator.

2.4.2 Solution Procedure

The dependent variables are the pressure, defined at the center of the primary cells, and the volume fluxes defined on the faces of the primary cells. This selection is equivalent to a finite-difference formulation over a staggered grid with the choice of scaled contravariant velocity components as the unknowns.

First the momentum equations are solved for an approximate U^l, which represents the volume-fluxes over the l-face of a computational cell. This is done by computing ΔU^l defined by

$$\Delta U^l = (U^l)^{n+1} - (U^l)^n$$

This first step velocity correction is obtained from the momentum equation by evaluating the pressure gradient term at time step (n). Various time advancing schemes can be implemented here. For example, an Adams-Bashforth type scheme used by Rosenfeld et al. (1988) can be written as follows

$$\left(V_{i+\frac{1}{2}}\, I - \Delta t D_l\right) \Delta \tilde{U}^l = \Delta t \left(\frac{3}{2} L_l^n - \frac{1}{2} L_l^{n-1} - R_\xi(\Delta P^{n-1}) - D_\xi(\Delta U^{\xi,n-1})\right) \qquad (2.16)$$

where D_l represents viscous terms, L the convection terms and R_l the pressure gradient terms.

In the second step, the velocity is updated such that the continuity equation is satisfied at the next time level. This is achieved by a single Poisson type equation as below:

$$D_{iv}\left(\frac{R_l(\phi)}{V_{m+\frac{1}{2}}}\right) = -D_{iv}\left((U^l)^n + \Delta \tilde{U}^l\right) \qquad (2.17)$$

Here, D_{iv} is a divergence-like operator defined by

$$D_{iv} U^l = U^\xi_{i+\frac{1}{2}} - U^\xi_{i-\frac{1}{2}} + U^\eta_{j+\frac{1}{2}} - U^\eta_{j-\frac{1}{2}} + U^\zeta_{n+\frac{1}{2}} - U^\zeta_{n-\frac{1}{2}}$$

Then, the variables at the new time level $n+1$ are computed from ΔU^l and the modified pressure, ϕ.

3. COMPUTED RESULTS

3.1 Code Development

In the previous chapter, solution methods based on pseudocompressibility and a fractional step approach have been described for 3-D applications in generalized coordinates. Several computer codes have been developed following these procedures. Each code is given a name listed as below. Results presented in the present paper will be identified with these names.

INS3D Code

A steady formulation of the pseudocompressibility approach is solved using an approximate factorization scheme. The spatial discretization utilizes second-order central differencing with additional numerical dissipation terms. The code has been validated. Numerous 3-D problems have been solved using this code.

INS3D-UP Code

This code is developed to obtain time-accurate solutions using the pseudocompressibility formulation. It is necessary to satisfy the continuity equation at each time step by subiteration in pseudotime. An upwind differencing scheme based on flux-difference splitting is used combined with an implicit line relaxation scheme. The code has been validated. Major unsteady flow applications of this code include the simulation of the flow through an artificial heart.

INS3D-LU Code

This code is also based on the pseudocompressibility formulation. However, a finite volume scheme in conjunction with either central or upwind differencing is used for spacial discretization. An LU-SGS implicit algorithm is employed for temporal discretization. This code has an option to utilize a rotating coordinate system so that rotor-steady state solutions (steady in a relative frame of reference) can be computed. The code is completely vectorized and validation is in progress in conjunction with the SSME turbopump flow analysis.

INS3D-FS Code

This code is based on a fractional-step method for computing time-accurate solutions. The

governing equations are discretized using a finite-volume approach on a staggered grid. A four-color ZEBRA scheme is devised for solving the Poisson equation for the pressure correction. The code validation is in progress.

3.2 Code Validation

Validation of some of the above flow solvers was done by choosing several basic configurations relevant to local flow encountered in problems of current interest such as the SSME power head. To remove uncertainties coming from turbulence modeling, the first validation cases were chosen in the laminar range of Reynolds numbers first, followed by turbulent case calculations. Examples are presented here.

Flow Over A Circular Cylinder

To represent an external flow, the flow past a circular cylinder was computed. Physically, for external flows, the pressure wave can quickly travel a short distance to balance the viscous region close to the body. The appropriate range of β in INS3D can be estimated based on this reasoning. In general, the magnitude of β is less restrictive for external flow than for internal flow. Several steady-state solutions were computed using the INS3D family of codes and showed good agreement with experiments and other computations (Kwak et al. 1986, Rogers and Kwak, 1988).

To capture the near field detail of transient flow, an impulsively started circular cylinder at Re=40 and 200 is computed using INS3D-FS code (see Rosenfeld et al., 1988, 1989). In Figure 1, time evolution of the separation length is compared with experiments by Coutanceau and Bouard (1977) and other computations by Collins and Dennis (1973). The comparison is very good.

As the Reynolds number increases above 40, a nonsymmetric wake develops and periodic vortex shedding sets in. Both INS3D-UP and INS3D-FS codes are validated using this problem. These computations are compared with other numerical and experimental results. Figure 2 shows a Strouhal number plot versus Reynolds number from computed results compared to experiments. Good agreement is observed.

The staggered pattern of the vortex shedding known as Karman's vortex street has been a subject of many flow visualization studies. For the purpose of comparison, particle traces are generated from the time-dependent solution of flow around a circular cylinder at a Reynolds number of 105 using the INS3D-UP (see Rogers and Kwak, 1988). In figure 3, this computed vortex street is shown on top. Shown in the bottom half of the figure is an

experimental photograph of the same conditions taken by S. Taneda and reproduced from Van Dyke (1982). The streaklines in the experiment are shown by electrolytic precipitation in water. The vortex structure is seen to be very similar between the two. The experimental picture is digitized and displayed on a workstation along with the computationally generated flow visualization picture.

Curved Duct of Square Cross-Section

The flow through a square duct with 90° bend offers a good test case for a full Navier-Stokes solver. This flow is rich in secondary flow phenomena both in the corner regions and through the curvature in the streamwise direction. This geometry was studied experimentally by Humphrey et al. (1977) and Taylor et al. (1981, 1982), and extensive laminar flow data are available. This particular geometry was used as a steady state test case for the INS3D family of codes. The geometry is shown in figure 4 and the Reynolds number of the flow is 790. The problem was non-dimensionalized using the side of the square cross-section. The inflow velocity was specified to be that of a fully developed, laminar, straight square duct (see White, 1974). The velocity is normalized by the average inflow velocity. The computed results are compared to the experimental results of Humphrey et al. (1977) as shown in figure 5. Overall, the comparison is quite satisfactory.

Extensive validation of the INS3D was performed by McConnaughey et al. (1989) utilizing the detailed inflow measurement by Taylor et al. (1981, 1982).

3.3 Space Shuttle Main Engine (SSME) Power Head Flow Simulation

Background

To increase the payload capability of the Space Shuttle, it is essential to understand the dynamics of the hot-gas flow in the engine power head. Because of the complexity of the geometry, an experimental approach is extremely difficult as well as time consuming. Computational simulation, therefore, offers an economical tool to complement the experimental work in analyzing the current configuration, and to suggest new, improved design possibilities.

The current arrangement for the SSME power head components is illustrated in figure 6. In the present staged combustion cycle, the fuel is partially burned at very high pressure and relatively high temperature in the preburners. The resulting hot gas is used to run the turbine. Hot gas discharged from the gas turbine passes through an annular 180° turn

before it diffuses into the fuel bowl. This assembly is called the hot gas manifold (HGM). The gas flows through transfer ducts into the main injector where, along with additional oxidizer, it is injected into the main combustion chamber. The Reynolds number of the primary flow in the manifold is of the order of 10^6 per inch. Because of the high gas temperature, the Mach number is less than 0.12. The flow is turbulent and is practically incompressible. As a part of the engine development effort, a CFD study has been conducted to simulate the dynamics of the hot-gas flow in the power head. Examples of the computed results presented in this section have been obtained using the INS3D code.

Computed Results

A computational model of the power head is chosen to analyze critical areas where the dynamics of the hot-gas flow are expected to have a significant effect on the overall performance of the SSME. As shown in figure 7, the model starts from the gas turbine exit on the fuel preburner side, and extends to the main injector assembly. The grid for the entire HGM system is generated by using algebraic functions, and is written with a high degree of flexibility to allow for changing geometric configurations.

For such a complicated turbulent flow as is encountered in the SSME, high level turbulence models such as a two-equation k-ϵ model or Reynolds-stress model may be needed. However, for many engineering applications, a simple yet adequately accurate algebraic model will be of considerable value for design purposes. Chang and Kwak (1988) devised a simple extended Prandtl-Karman mixing length theory which, together with the strength of the vorticity, forms an eddy viscosity model. This model has been used for the present simulation.

Extensive computational flow analysis was performed to identify the areas of potential improvement. From this computational flow analysis and also from experiments, the center duct of the current three-transfer-duct HGM is found to transfer a limited amount of mass (about 10% of the total flow). Also the transverse pressure gradient remains large and a large separation bubble is observed after the 180° turn. To improve the quality of the flow, a large-area, two-duct design concept has been developed. Then, to reduce the large separation bubble after the 180° turn, over 20 different two-duct configurations were studied computationally, thereby providing potentially the optimum geometry to the designers.

The turbulent solution for the new two-duct HGM is compared to that of experiments performed using both the current three-duct HGM and the new two-duct configuration. As shown in figure 8, the pressure gradient around the fuel bowl of the HGM is greatly

reduced from that of the original configuration. From the hardware perspective, this results in substantially reduced loads on the bearings which hold the gas turbine and the turbopump.

The most significant objective of the present study is to pinpoint the locations where flow experiences the most energy losses. An important measure of the energy losses is the mass-weighted average total pressure along the flow. Figure 9 illustrates the decreasing coefficient of the mass-weighted total pressure along the centerline of the turnaround duct, the fuel bowl, and the transfer duct. In the figure, three different HGM configurations are compared. The initial two-duct design shows 28% less total pressure drop than the current three-duct version. After the two-duct configuration was fine-tuned computationally, the pressure drop decreased even further to 36% less than the original configuration. This final configuration is then tested using cold air flow, which showed a 40% reduction in pressure loss. This example illustrates the value of CFD in aerospace design. More detailed informaion can be found in our earlier publications (see Chang et al. 1988, Yang et al. 1987, Kwak 1989)

3.4 Artificial Heart Flow Simulation

Background

Recently, the demand for mechanical hearts or ventricular-assist devices (VAD) as a temporary life support system has grown. These devices are becoming powerful tool for assisting patients to recover from heart attacks or as a temporary bridge to transplants. A research and development effort is in progress to improve the flow quality in these devices as well as to develop better materials and control systems. Experimental investigations on these devices are very limited and many aspects of the flow in the devices are yet to be studied. Therefore, it will be very valuable to medical researchers to simulate the flow by applying state-of-the-art CFD technology (see, for example, Peskin, 1982).

Blood flow through these mechanical devices is very complicated in many respects. The fluid may exhibit significant non-Newtonian characteristics locally and the geometry is usually very complicated. In an artificial organ, as red blood cells go through high shear turbulence regions, they may be damaged; the downstream region of an artificial heart valve is an example. The flow is unsteady, possibly periodic, incompressible and very viscous. This problem is very much interdisciplinary so an attempt for a complete simulation would be a very formidable task. However, an analysis based on a simplified model may provide much needed physical insight into the blood flow through these devices.

The formulation of the flow solvers described earlier in this paper is based on a Newtonian fluid assumption. However, since the governing equations are solved in a generalized coordinate system, viscosity that varies in space and time, as well as a moving geometry, is allowed. The primary purpose of the current application is to demonstrate that technology developed for aerospace can be extended to biofluid analysis. Among many variations, the present demonstration calculation is being performed on the Penn State artificial heart (Tarbell et al., 1986). In the computational simulation, the time-accurate INS3D-UP code is used.

Computed Results

The actual model of the Penn State artificial heart poses some very difficult problems from a computational stand point. A schematic and a computer model of the heart are shown in figures 10 and 11, respectively. The heart is composed of a cylindrical chamber with two openings on the side for valves. The pumping action is provided by a piston surface which moves up and down inside the chamber. The actual heart has a cylindrical tube extending out of each of the valve openings. These tubes contain tilting flat disks which act as the valves. The current computational model will neglect the valves altogether and will use the right and left openings shown in

figure 11 for the inflow and outflow boundaries, respectively. In the computations, as the piston reaches topmost position, the outflow valve closes and the inflow valve will open instantaneously. Similarly, as the piston reaches its bottommost position, the outflow valve will open and the inflow valve will close.

The calculations were carried out on a Cray 2 supercomputer with an H-H grid topology and grid dimensions of 39 x 39 x 51. The computations started with the fluid at rest, the piston at the bottom position, and the outflow valve open. The velocity of the piston during the period of motion between its maximum and minimum positions was set to be constant, which is very nearly the same as that in the actual heart device. The period of the entire piston cycle was set to a time of five non-dimensional units, and the time step was chosen so that 200 physical time steps were required for each full cycle of the piston.

Some very interesting flow physics occurred during this period of motion. Various post-processing techniques have been utilized in analyzing the results, such as velocity vectors colored by pressure level and vorticity magnitude contours which can be related to the wall shear stress. Figure 12a shows particle traces as the piston nears its bottomposition. Two distinct vortices are seen to have formed from the flow separation that occurs as it enters through the inflow valve. In figure 12b, an experimental photograph (J.M. Tarbell,

Pennsylvania State University, private communication, 1988) shows bubbles entering the inflow valve as the piston nears its bottomposition. A similar two-vortex system is seen to form here.

The present solution shows the capability of the computational procedure for simulating complicated internal flows with moving boundaries. For this initial calculation, the motion of the piston of the actual device was simplified. Also neglected was the valve opening and closing, which will be simulated in the future. This work represents simply the first step toward developing a CFD tool for this type of flow.

4. CONCLUDING REMARKS

In the present paper, numerical simulation methods for viscous incompressible flows are discussed from an application point of view. Our main interest has been in three-dimensional real-world geometries. Naturally, the computational requirements for these problems are different from fundamental fluid dynamics studies. Therefore, the main emphasis has been placed on a primitive variable formulation, which has been the most commonly used approach for three-dimensional problems to date.

In a practical sense, even though computer speed and memory have been increased substantially in the recent past, the speed and memory requirements of a flow solver are still dictated by the turnaround time. In many engineering applications, it is very important to generate solutions in a timely fashion to make an impact on the design and analysis. We feel that numerical simulations can now provide complementary information to measured data, thus reducing the number of experimental trials required for developing advanced flow devices. A more sophisticated approach, such as computer optimization of a design can be attempted when the flow solver becomes at least one order of magnitude faster or the computer speed can be improved that much, perhaps by through use of massive parallelism.

There are several areas to be considered in developing a new generation of fast flow solvers. Several additions to the technology presented here will help to make the current methods as efficient as possible. Multigrid acceleration is one possibility which is physically consistent with the incompressible formulation. Overall, the solution procedure should be developed to best utilize computer characteristics such as vectorization, parallel processing, and access to memory.

In the development of a universal code, it is hard to devise the best scheme for all flow

speeds and for many different types of flow. Because of the uncertainties related to the turbulence model, it seems better to have a specialized code suitable for each class of problems. For example, one can imagine having a code for an impeller-type problem while having another for flow over aerodynamic shapes. Despite the limitations in algorithm speed and accuracy and computer speed and memory, when the state-of-the-art flow solvers are combined with creative researchers, the result will be tremendously beneficial for developing modern devices requiring viscous incompressible flow analysis.

REFERENCES

Beam, R. M., and Warming, R. F., "An Implicit Factored Scheme for the Compressible Navier-Stokes Equations,"AIAA J., vol. 16, pp. 393-402, 1978.

Braza, M., Chassaing, P., and Ha Minh, H., "Numerical Study and Physical Analysis of the Pressure and Velocity Fields in the Near Wake of a Circular Cylinder," J. Fluid Mech., vol. 165, pp. 79-130, 1986.

Caretto, L.S., Gosman, A.D., Patankar, S.V., and Spalding, D.B., "Two Calculation Procedures for Steady Three-Dimensional Flows with Recirculation,"Proceedings of the 3rd Int. Conference on Numerical Methods in Fluid Dynamics, Paris, France, p. 60, 1972.

Chakravarthy, S. R., and Osher, S., "A New Class of High Accuracy TVD Schemes For Hyperbolic Conservation Laws," AIAA Paper 85-0363, 1985.

Chang, J. L. C., and Kwak, D., "On the Method of Pseudo Compressibility for Numerically Solving Incompressible Flows,"AIAA Paper 84-0252, 1984.

Chang, J. L. C. and Kwak, D., "Numerical Study of Turbulent Internal Shear Layer Flow in an Axisymmetric U-Duct,"AIAA Paper 88-0596, 1988.

Chang, J.L.C., Kwak, D., Rogers, S. E., and Yang, R-J, "Numerical Simulation Methods of Incompressible Flows and an Application to the Space Shuttle Main Engine,"Int. J. Numerical Method in Fluids, vol. 8, pp. 1241-1268, 1988.

Choi, D. and Merkle, C.L., "Application of Time-Iterative Schemes to Incompressible Flow,"AIAA J., vol. 23, no. 10, 1518-1524, 1985.

Chorin, A. J., "A Numerical Method for Solving Incompressible Viscous Flow Problems,"J. Comp. Phys., vol. 2, pp.12-26, 1967.

Chorin, A.J., "Numerical Solution of Navier-Stokes Equations,"Mathematics of Computation, vol. 22, No. 104, 745-762, 1968.

Collins, W. M. and Dennis, S. C. R., "Flow Past an Impulsively Started Circular Cylinder," J. Fluid Mech., vol. 60, pp. 105–127, 1973.

Coutanceau, M. and Bouard, R., "Experimental Determination of the Main Features of the Viscous Flow in the Wake of a Circular Cylinder in Uniform Translation. Part 2. Unsteady Flow," J. Fluid Mech., vol. 79, pp. 257–272, 1977.

Dwyer, H.S., Soliman, M., and Hafez, M., "Time Accurate Solutions of the Navier-Stokes Equations for Reacting Flows,"Proceedings of the 10th Int. Conference on Numerical Methods in Fluid Dynamics, Beijing, China, pp. 247-251, Springer-Verlag, June 1986.

Ferziger,J.H., "Incompressible Turbulent Flows,"J. Comp. Phys., vol. 69, pp. 1-48, 1987.

Gresho, M. P. and Sani, R. L., "On Pressure Boundary Conditions for the Incompressible Navier–Stokes Equations," Int. J. Numerical Methods in Fluids, vol. 7, pp. 1111–1145, 1987.

Harlow, F. H. and Welch, J. E., "Numerical Calculation of Time-Dependent Viscous Incompressible Flow with Free Surface," Phys. Fluids, vol. 8, No. 12, pp. 2182-2189, Dec. 1965.

Harten, A., Lax, P. D., and Van Leer, B., "On Upstream Differencing and Godunov-Type Schemes for Hyperbolic Conservation Laws," Siam Review, vol. 25, No. 1, p. 35, 1983.

Humphrey, J. A. C., Taylor, A. M. K., and Whitelaw, J. H., "Laminar Flow in a Square Duct of Strong Curvature," J. Fluid Mech., vol. 83, part 3, pp. 509–527, 1977.

Kim, J. and Moin, P., "Application of a Fractional-Step Method to Incompressible Navier-Stokes Equations," J. Comp. Phys., vol. 59, pp. 308–323, 1985.

Kwak, D., Chang, J. L. C., Shanks, S. P., and Chakravarthy, S., "A Three-Dimensional Incompressible Navier-Stokes Flow Solver Using Primitive Variables,"AIAA J, vol. 24, No. 3, 390-396, Mar. 1986

Kwak, D., "Computation of Viscous Incompressible Flows,"von Karman Institute for Fluid Dynamics, Lecture Series 1989-04, Mar. 6-10, 1989

MacCormack, R. W., "Current Status of Numerical Solutions of the Navier-Stokes Equations," AIAA Paper 85-0032, 1985.

Marchuk, G.M., Methods of Numerical Mathematics, Springer-Verlag, 1975.

McConnaughey, P., Cornelison, J., and Barker, L. "The Prediction of Secondary Flow in Curved Ducts of Square Cross-Section,"AIAA Paper 89-0276, 1989,

Merkle, C. L. and Athavale, M., "Time-Accurate Unsteady Incompressible Flow Algorithms Based on Artificial Compressibility," AIAA Paper 87-1137, 1987.

Orszag, S. A., and Israeli, M., "Numerical Simulation of Viscous Incompressible Flows," Annual Rev. Fluid Mech., vol. 6, 1974.

Orszag, S. A., Israeli, M. and Deville, M.O., "Boundary Conditions for Incompressible Flows," J. Scientific Computing, vol. 1, pp. 75–111, 1986.

Patankar, S. V. and Spalding, D. B., "A Calculation Procedure for Heat, Mass and Momentum Transfer in Three–Dimensional Parabolic Flows," Int. J. Heat and Mass Transfer, vol. 15, pp. 1787–1806, 1972.

Patankar, S.V., "Numerical Heat Transfer and Fluid Flow,"Hemisphere Publishing Co., New York, 1980.

Peskin, C. S., "The Fluid Dynamics of Heart Valves: Experimental, Theoretical and Computational Methods," Ann. Rev. Fluid Mech., vol. 14, pp. 235–259, 1982.

Roe, P. L., "Approximate Riemann Solvers, Parameter Vectors, and Difference Schemes," J. Comput. Phys., vol. 43, p. 357, 1981.

Roach, P.J., Computational Fluid Dynamics, Hermosa Publishers, Albuquerque, NM, 1972.

Rogers, S. E. and Kwak, D., "An Upwind Differencing Scheme For the Time-Accurate Incompressible Navier-Stokes Equations," AIAA Paper 88-2583, 1988.

Rogers, S. E. and Kwak, D., "Numerical Solution of the Incompressible Navier-Stokes Equations for Steady and Time-Dependent Problems,"AIAA Paper 89-0463, 1989.

Rosenfeld, M., Kwak, D. and Vinokur, M., "A Solution Method for the Unsteady and Incompressible Navier-Stokes Equations in generalized Coordinate Systems,"AIAA Paper 88-0718, 1988.

Rosenfeld, M., and Kwak, D., "Numerical Solution of Unsteady Incompressible Flows in Generalized Moving Coordinate Systems,"AIAA Paper 89-0466, 1989.

Steger, J. L. and Kutler, P., "Implicit Finite-Difference Procedures for the Computation of Vortex Wakes,"AIAA J. vol. 15, no. 4, pp. 581-590, Apr. 1977.

Steger, J. L., and Warming, R. F., "Flux Vector Splitting of the Inviscid Gasdynamic Equations With Application to Finite Difference Methods," J. Comp. Phys., vol. 40, no. 2, pp. 263-293, 1981.

Tarbell, J. M., Gunshinan, J. P., Geselowitz, D. B., Rosenburg, G., Shung, K. K., and Pierce, W. S., "Pulse Ultrasonic Doppler Velocity Measurements Inside a Left Ventricular Assist Device," J. Biomech. Engr., Trans. ASME, vol. 108, pp. 232–238, 1986.

Taylor, A.M.K.P., Whitelaw, J.H., and Yianneskis, M., "Measurements of Laminar and Turbulent Flow in a Curved Duct with Thin Inlet Boundary Layers,"NASA CR-3367, Jan. 1981.

Taylor, A.M.K.P., Whitelaw, J.H., and Yianneskis, M., "Curved Ducts with Strong Secondary Motion: Velocity Measurements of Developing of Laminar and Turbulent Flow,"J. Fluid Engineering, vol. 104, pp. 350-359, Sept. 1982.

Van Dyke, M., An Album of Fluid Motion, The Parabolic Press, Stanford, Calif. 1982.

White, F. M., Viscous Fluid Flow, McGraw-Hill, New York, NY, p. 123, 1974.

Yanenko, N.N., The Method of Fractional Steps, Springer-Verlag, Berlin, 1971.

Yang, R-J, Chang, J. L. C., and Kwak, D., "A Navier-Stokes Simulation of the Spce Shuttle Main Engine Hot Gas Manifold ,"AIAA Paper 87-0368, 1987.

Yoon, S. and Jameson, A., "An LU-SSOR Scheme for the Euler and Navier-Stokes Equations,"AIAA Paper 87-0600, 1987.

Yoon, S. and Kwak, D., "Artificial Dissipation Models for Hypersonic External Flow,"AIAA Paper 88-3708, 1988.

Yoon, S. and Kwak, D., "LU-SGS Implicit Algorithm for Three-Dimensional Incompressible Navier-Stokes Equations with Source Term,"AIAA Paper 89-1964, AIAA 9th Computational Fluid Dynamics Conference, Buffalo, NY, June 14-16, 1989.

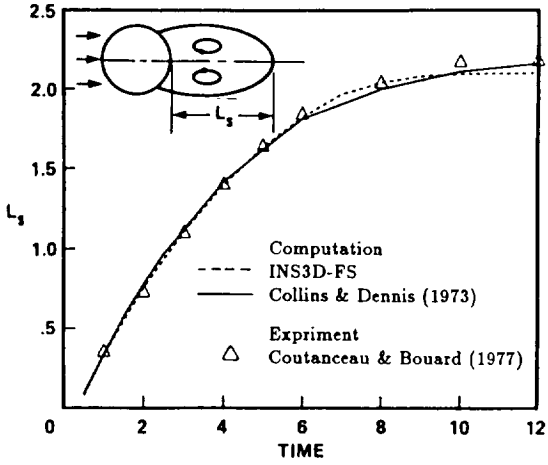

Figure 1.-Time evolution of separation length for flow over a cylinder at Re=40.

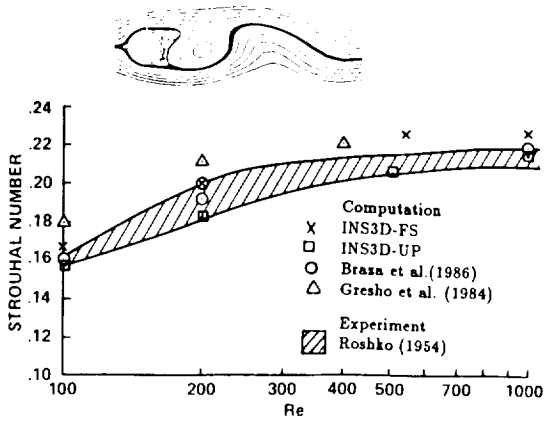

Figure 2.-Vortex shedding from a circular cylinder.

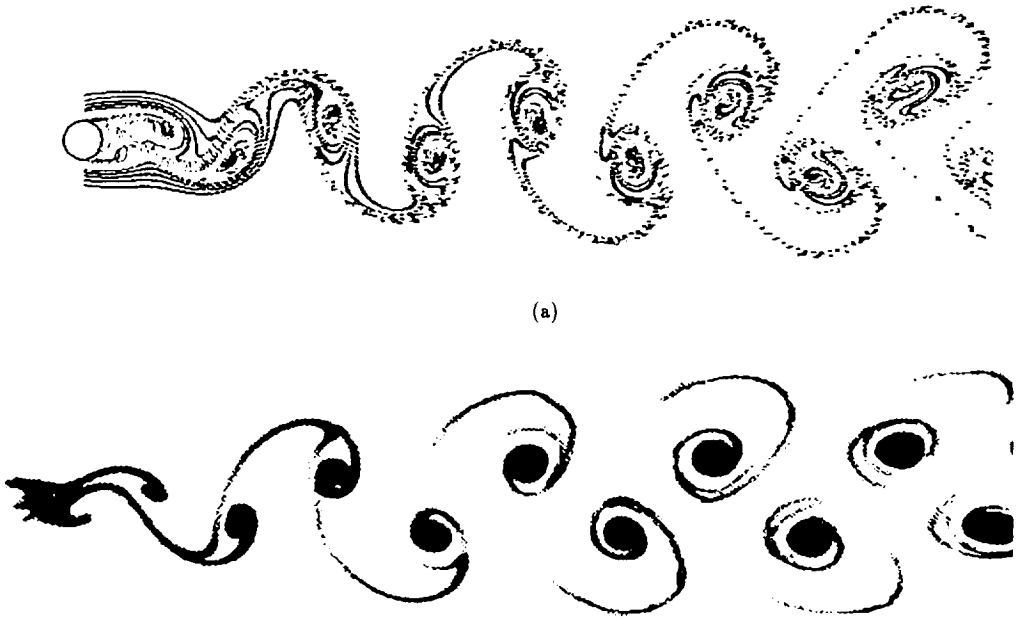

Figure 3.-Karman vortex street behind a circular cylinder at Re=105: (a) computed (INS3D-UP). (b) experiment (S. Taneda, from Van Dyke, 1982).

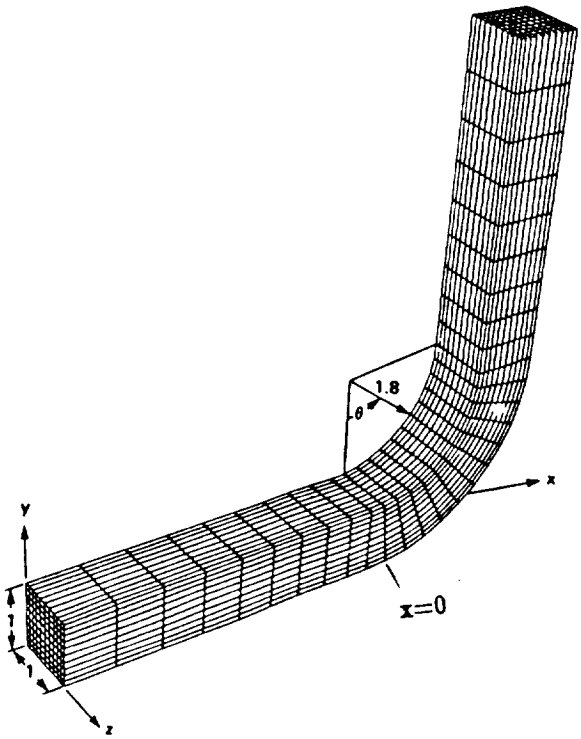

Figure 4.-Geometry of a square duct with 90° bend.

Computation (41x21x21 grid)
---- INS3D-UP
—·— INS3D-LU
—— INS3D-FS

Experiment
\+ Humphrey et al. (1977)

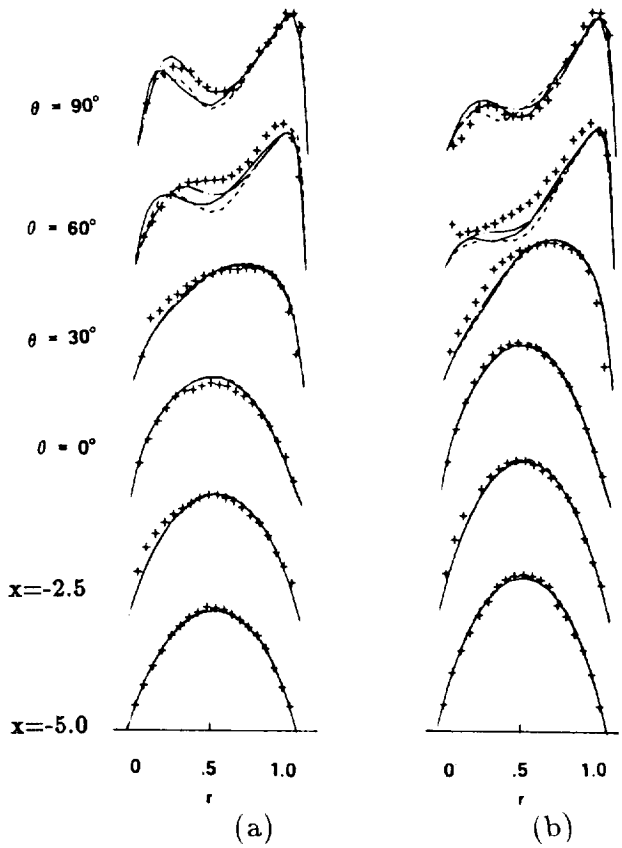

Figure 5.-Streamwise velocity profile for flow through a 90° bend at Re=790 : (a) xy-plane at z=0.25. (b) xy-plane at z=0.5

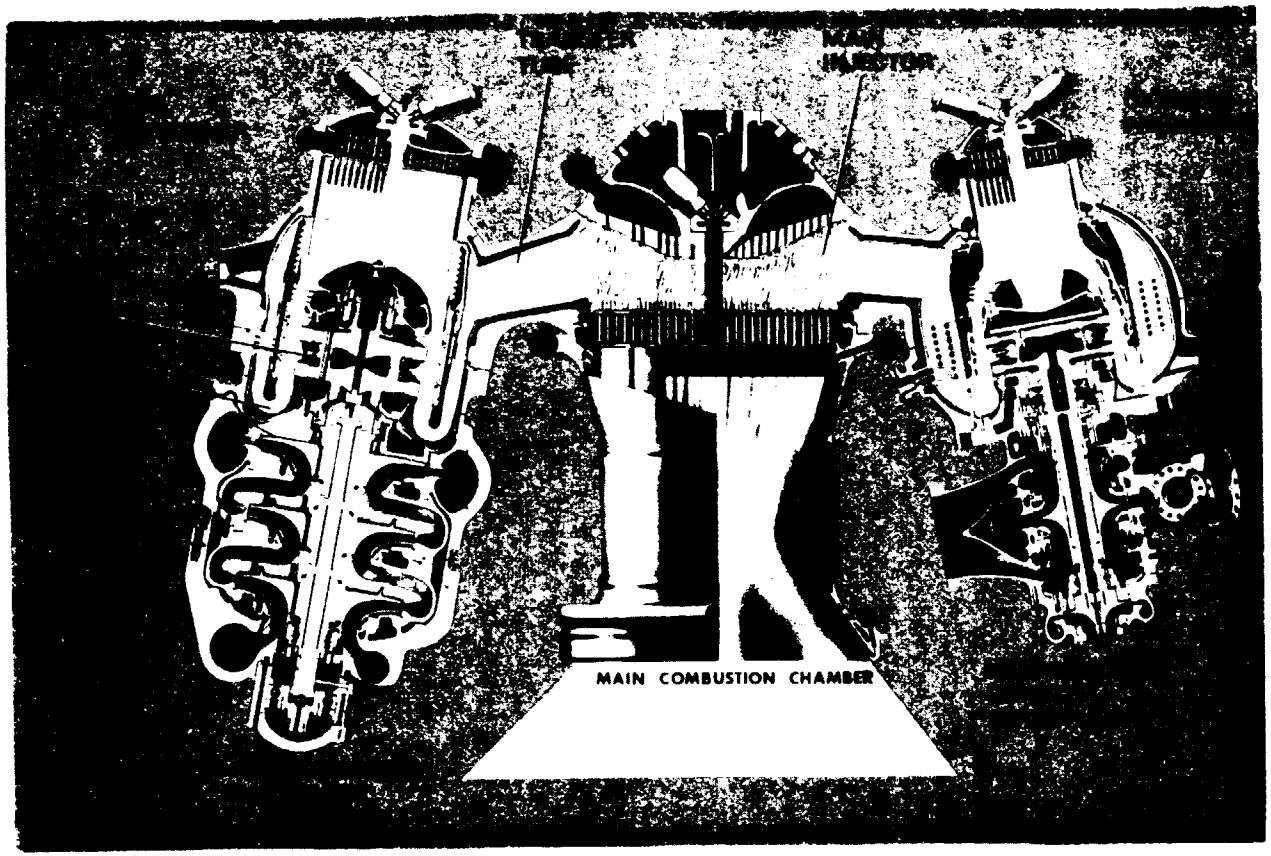

Figure 6.-SSME power head component arrangement.

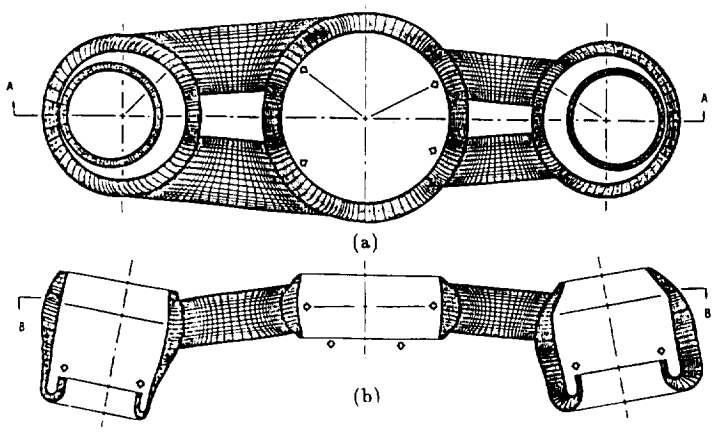

Figure 7.-Computer model of the new two-duct SSME power head. (a) vertical cross-section (B-B). (b) horizontal cross-section (A-A).

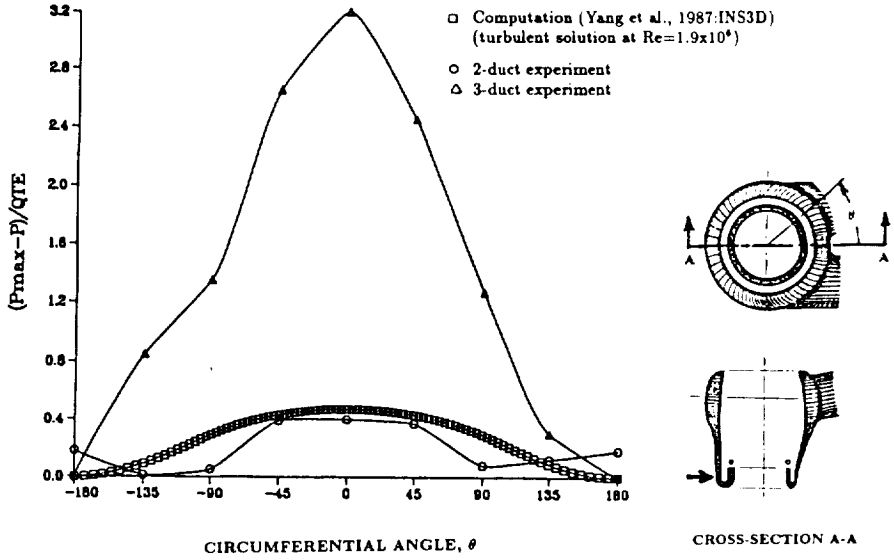

Figure 8.-Pressure coefficient on fuel bowl outer surface after 180° turn.

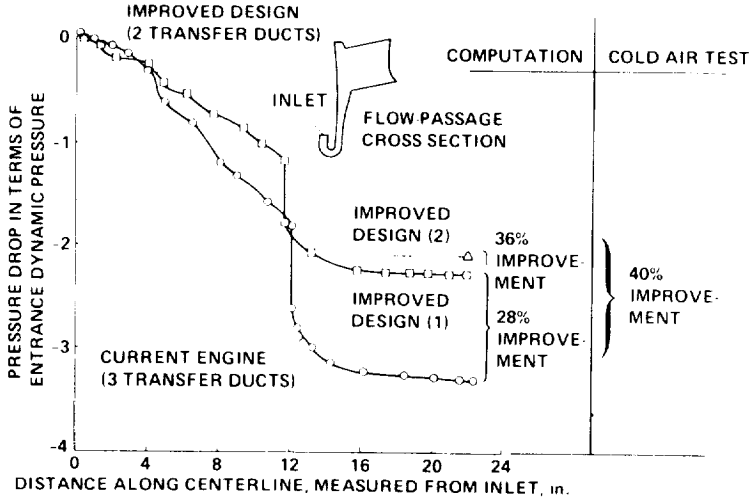

Figure 9.-Pressure losses in three-duct and two-duct HGM.

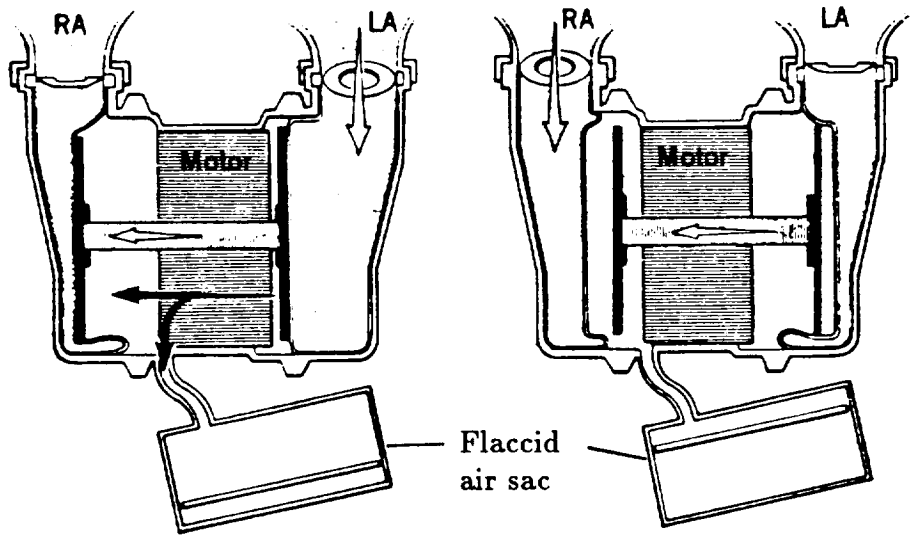

Figure 10.-Schematic of the electric motor driven Penn State artificial heart.

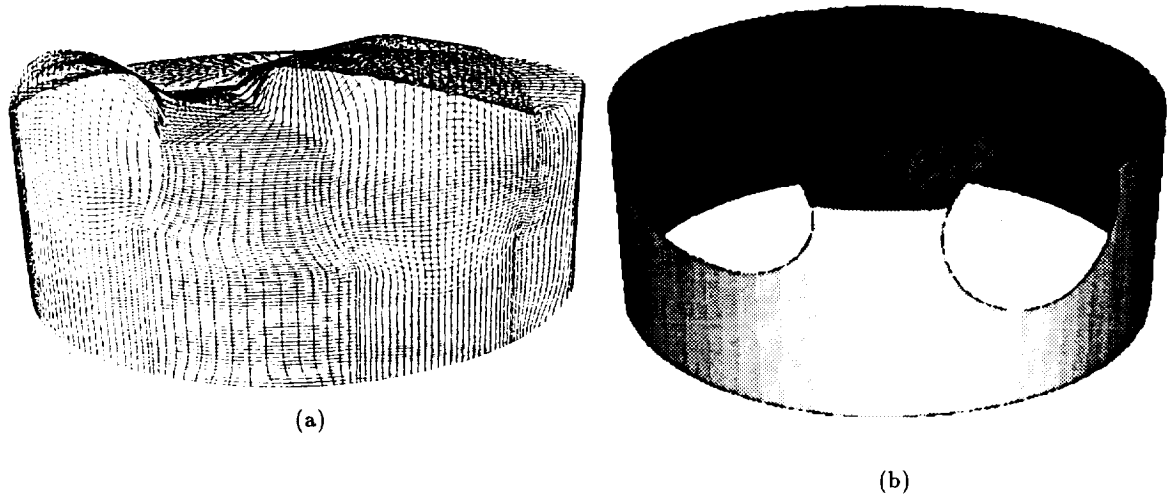

Figure 11.-A computer model of the Penn State artificial heart:
(a) surface grid. (b) main chamber showing valve openings.

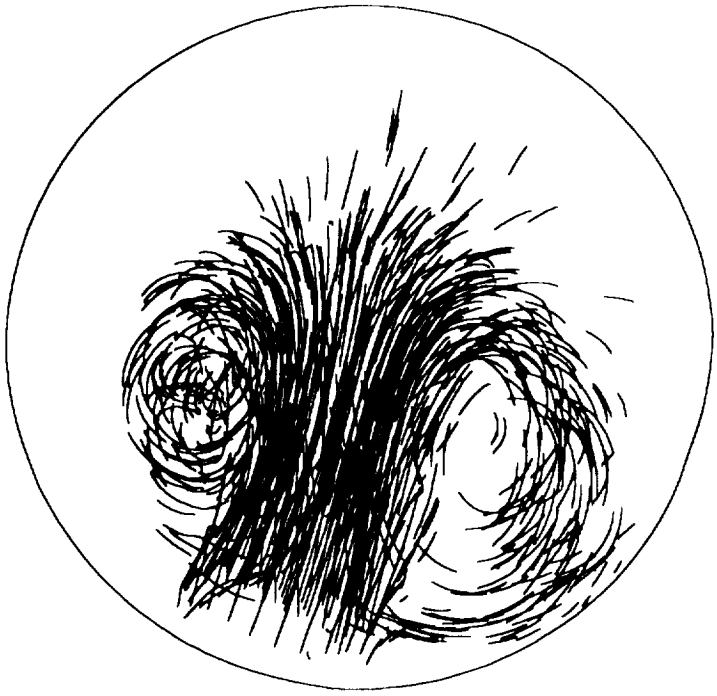

a. Computational results

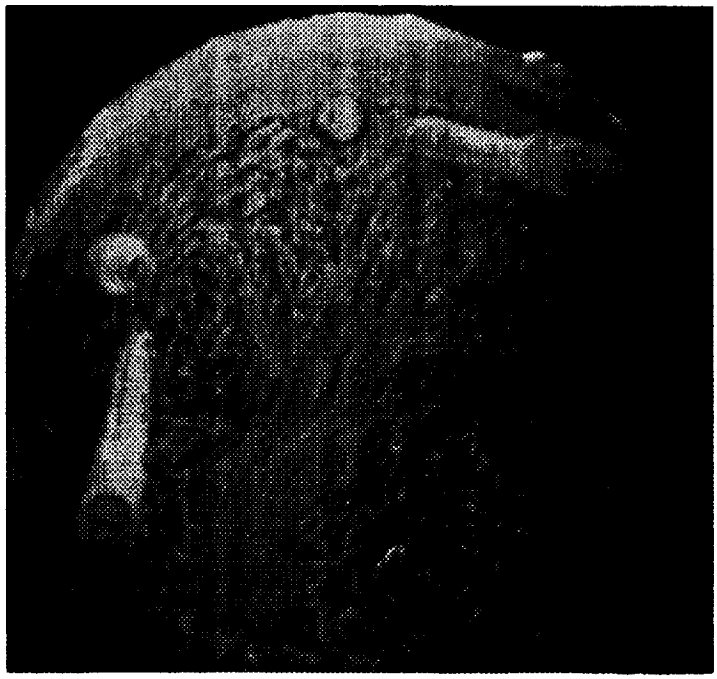

b. Experimental results

Figure 12.-Incoming particle traces as the piston nears the bottommost position: (a) computation (Rogers et al., 1989). (b) experiment (J.M. Tarbell, Pennsylvania State University, 1988).

NASA
National Aeronautics and Space Administration

Report Documentation Page

1. Report No.	2. Government Accession No.	3. Recipient's Catalog No.
NASA TM-102202		

4. Title and Subtitle

Numerical Simulation of Viscous Incompressible Flows

5. Report Date

September 1989

6. Performing Organization Code

7. Author(s)

D. Kwak, S. Rogers, S. Yoon, M. Rosenfeld, and J. L. C. Chang
(Rocketdyne, Rockwell International, Canoga Park, CA)

8. Performing Organization Report No.

A-89174

10. Work Unit No.

505-60-01

9. Performing Organization Name and Address

Ames Research Center
Moffett Field, CA 94035

11. Contract or Grant No.

13. Type of Report and Period Covered

Technical Memorandum

12. Sponsoring Agency Name and Address

National Aeronautics and Space Administration
Washington, DC 20546-0001

14. Sponsoring Agency Code

15. Supplementary Notes

Point of Contact: Dochan Kwak, Ames Research Center, MS 258-1, Moffett Field, CA 94035
(415) 694-6743 or FTS 464-6743

Presented at the U.S.-Korea Joint Seminar on Fluid Engineering and Science, Seoul, Korea, September 3-9, 1989.

16. Abstract

This paper discusses incompressible Navier-Stokes solution methods and their applications to three-dimensional flows. A brief review of existing methods is given followed by a description of recent progress on development of three-dimensional generalized flow solvers. Emphasis is placed on primitive variable formulations which are most promising and flexible for general three-dimensional computations of viscous incompressible flows. Both steady- and unsteady-solution algorithms are discussed. Finally, examples of real world applications of these flow solvers are given.

17. Key Words (Suggested by Author(s))

Incompressible flow
Navier-Stokes equations
Finite differences

18. Distribution Statement

Unclassified-Unlimited

Subject Category - 34

19. Security Classif. (of this report)	20. Security Classif. (of this page)	21. No. of Pages	22. Price
Unclassified	Unclassified	27	A03